

The Properties of PVA-Cockle Shell Derived Hydroxyapatite Synthesized through Wet Chemical Precipitation Method

Anis Fadhilla Azhar¹, Nur Hezreen Najwa Abdul Muizz¹,
Natasha Ahmad Nawawi^{1,2*}

¹Faculty of Mechanical Engineering, Universiti Teknologi MARA (UiTM), 40450 Shah Alam, Selangor Darul Ehsan, Malaysia

²Engineered Materials and Structures Research Group, Faculty of Mechanical Engineering, Universiti Teknologi MARA (UiTM), 40450 Shah Alam, Selangor Darul Ehsan, Malaysia

ARTICLE INFO

Article history:

Received 28 July 2025

Revised 27 August 2025

Accepted 28 August 2025

Online first

Published 15 September 2025

Keywords:

Hydroxyapatite

Biogenic source

Cockle shell

Wet precipitation

Polyvinyl alcohol

DOI:

<https://doi.org/10.24191/jmeche.v22i3.8194>

ABSTRACT

The increasing demand for biocompatible materials in medical applications has driven the search for sustainable and low-cost sources of hydroxyapatite (HA), a major component of bone and teeth. Conventional HA synthesis relies on expensive or non-renewable calcium sources, which has highlighted the need for alternative, eco-friendly precursors. This study aims to investigate the potential of cockle shells, an abundant biogenic waste material, as a calcium precursor for the synthesis of HA via the wet precipitation method. In addition, incorporating additives such as polyvinyl alcohol (PVA) is proposed to investigate the effects of PVA addition on the chemical and physical properties of synthesized HA, especially in terms of its homogeneity and structural purity. Cockle shells in the form of calcium oxide (CaO) were mixed with diammonium hydrogen phosphate to form HA via the wet precipitation method. Thermogravimetric analysis (TGA) indicated 750 °C as the minimal conversion temperature from CaCO₃ to pure CaO. The obtained CaO was then reacted with diammonium hydrogen phosphate (NH₄)₂HPO₄ to produce HA. Subsequently, PVA was added to synthesized HA with various concentrations (2.5 wt%, 5.0 wt%, and 7.5 wt%) followed by a heat treatment at 1000 °C, which later known as HAP samples. X-ray Diffraction (XRD) and Fourier Transform Infrared Spectroscopy (FTIR) analysis verifies HA formation with a clear peak at 31.8° with the lowest crystallite size of 436.74 nm at HAP 3 (7.5 wt% PVA) and functional groups of phosphate and hydroxyl bands, respectively. Besides that, Scanning Electron Microscopy (SEM) shows that HAP 3 (7.5 wt% PVA) resulted in the spherical morphology with a less agglomerated particle size of 0.172 µm. Overall, calcium source from cockle shells has been successfully employed in producing HA. The addition of 7.5 wt% PVA (HAP 3) successfully enhanced the structural properties of HA as PVA acted as a stabilizing and dispersing

^{1*} Corresponding author. E-mail address: natashanawawi@uitm.edu.my
<https://doi.org/10.24191/jmeche.v22i3.8194>

agent, improving crystallinity, preserving functional groups, and reducing particle agglomeration.

INTRODUCTION

Hydroxyapatite (HA) with the chemical formula, $\text{Ca}_{10}(\text{PO}_4)_6(\text{OH})_2$ is a mineral form of calcium phosphate that is like the mineral of bones and teeth in humans and is also a widely used biomaterial due to its excellent bioactivity and biocompatibility (Sirisoam et al., 2018; Kati et al., 2022). Although hydroxyapatite, has poor mechanical properties, it is an extremely strong material for tissue engineering (Abifarin et al., 2023; Redhwi et al., 2024). As a result, HA composites that include metals, polymers or other reinforcing agents have been created to enhance mechanical qualities while maintaining biological functionality. However, expensive and non-renewable precursors are usually needed for the synthesis of HA, which might limit its wide application (Rosley et al., 2024). Hence, the use of natural precursors from biogenic CaCO_3 sources has increased in demand as it not only helps in waste management but also provides an affordable and sustainable way to produce HAP for various applications, including bone tissue engineering and as a catalyst in environmental processes. Literally, HA can be prepared by several techniques, such as sol-gel, microwave-assisted, and wet precipitation. It was reported that HA prepared by the sol-gel method at room temperature offers control in particle size (Ng et al., 2022), however, it requires a long and laborious process. Meanwhile, microwave-assisted synthesis uses microwave radiation to rapidly heat the reactants, significantly speeding up the formation of HA (Cruz-Avila et al., 2024). However, in this work, attempts were made to use the wet precipitation method in the HA formation due to its simplicity, low cost and appropriateness for future mass-scale HA production. Besides that, this method enables the fine-tuning of particle size and crystallinity by utilizing a controlled reaction between calcium precursors and a phosphate source.

PVA is a synthetic polymer with hydrophilic, flexible and biocompatible properties, and it has shown great potential to reinforce HA in strength, toughness and porosity (Italiano et al., 2024). Studies that worked on binding PVA to HA composites have collectively reported that PVA has facilitated the interfacial bonding between the HA particles and hence has indirectly improved its mechanical performance (Anggresani et al., 2023; Novella et al., 2023; Shalygina et al., 2024). This composite ability to retain water helps to control its porosity, which is crucial for tissue engineering and bone scaffolds, as a porous structure allows proper nutrient flow and cell growth (Novella et al., 2023). Hence, it is expected that with proper adjustment of the PVA concentration, the strength structure of this composite can be optimized, making it suitable for load-bearing applications. Besides that, it was reported that HA-PVA composites have obtained good behaviour as a coating of implants and scaffolds in bone generation applications (Shalygina et al., 2024). However, challenges remain in achieving uniform PVA distribution within the HA matrix and maintaining consistent structural properties. Despite this, adding PVA still shows great potential for improving HA performance in biomedical applications.

Additionally, sintering is the key process that enhances HA-PVA composites as the sintering conditions control the material's final structure, including grain size, crystallinity, porosity and crystal formation (Cahyaningrum et al., 2018; Abifarin et al., 2023; Trzaskowska et al., 2023; Redhwi et al., 2024). This consequently improves density, strength and hardness and reduces pores by bonding these particles together (Priwintoko et al., 2023). These properties make this material suitable for load-bearing applications such as dental implants and bone scaffolds (Khiri et al., 2016; Abifarin et al., 2023).

In summary, this study intends to provide an environmentally friendly and sustainable method of producing HA via using the wet precipitation method to synthesize HA from calcium carbonate obtained from cockle shells. To further increase the synthetic HA potential for use in biomedical applications, the study additionally investigates how PVA affects the material's structural, morphological and crystallinity

characteristics. In this project, the process uses a different concentration of polyvinyl alcohol (2.5 wt%, 5 wt%, and 7.5 wt%). Through investigating these objectives, this study helps assist in developing biocompatible materials from natural sources and enhances their qualities by adding polymers, paving the way for improved bone graft substitutes and other medical uses.

METHODOLOGY

Fig 1 shows the flowchart of processes involved in preparing HA-PVA composites. The methodology employed is discussed in detail below.

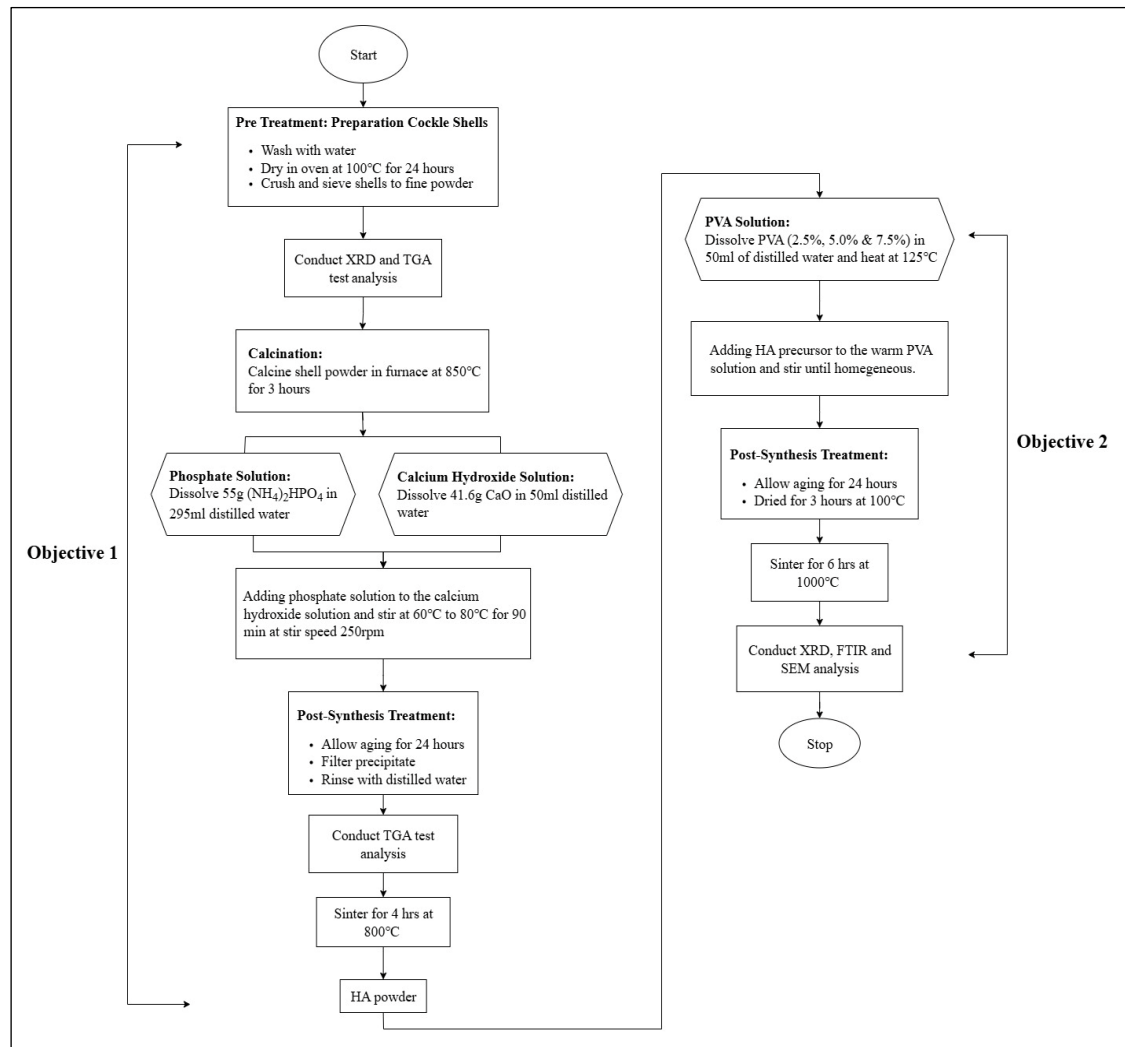


Fig. 1. Flowchart of the overall process HA-PVA derived using CaO from cockle shell.

Pre-Treatment of Cockle Shells

The biogenic waste, which was cockle shells, was collected at the restaurant, and the impurities were removed. The uncrushed cockle shells were cleaned with water. The cleaned shells were oven-dried at 100 °C and sun-dried for one day. After that, the dried cockle shells were crushed using a mortar and blender and the shells were sieved to produce the fine powder.

Synthesis of Hydroxyapatite

The cockle shell powder was calcined at 850 °C for 3 hours in a furnace. After that, 41.6 g of calcium oxide (CaO) was added to 50 ml of distilled water and 55 g of diammonium hydrogen phosphate (NH₄)₂HPO₄ was dissolved in 295 ml of distilled water with a molar ratio of Ca/P = 1.67. Then, both solutions were mixed under stirring. By continuously monitoring the reaction pH remained within an acceptable range (pH 9–11) using a pH meter to favour the formation of hydroxyapatite. The resulting precipitate was filtered, rinsed with distilled water and dried at 100 °C for 24 hours.

Synthesis of HA-PVA

Table 1 shows the different weight ratios of the HA and PVA mixture used in this research. The PVA powder was dissolved at different concentrations (2.5 wt%, 5.0 wt%, and 7.5 wt% of HA total weight) in 50 ml of distilled water by heating at 125 °C with continuous stirring using a magnetic stirrer. Then, the 5g HA (100 wt%) was slowly added to the warm PVA solution while stirring continuously until a homogeneous slurry was formed. After that, the mixture was dried at 100 °C for 2 hours, followed by sintering the resulting precipitate at 1000 °C for 6 hours. The synthesized hydroxyapatite samples were labelled as HAP 1 (HA-2.5 wt% PVA), HAP 2 (HA-5.0 wt% PVA), and HAP 3 (HA-7.5 wt% PVA).

Table 1. Weight ratio of HA-PVA mixture

	Hydroxyapatite (HA)	Polyvinyl Alcohol (PVA)
HAP 1 (2.5%)	5.0 g	0.125 g
HAP 2 (5.0%)	5.0 g	0.250 g
HAP 3 (7.5%)	5.0 g	0.375 g

Characterization

The HA-PVA composite was characterized using X-Ray Diffraction (XRD) to confirm its crystalline structure and crystallite size of HA. This analysis was carried out at room temperature, operated at 45 kV and 40 mA using Cu-K α as the radiation source. The X-ray step size was 0.026° with the scan angle (2 θ) varying from 10° to 60°. The crystallite size of the powder was calculated using the Scherrer equation, as shown in Equation 1. Next, Fourier Transform Infrared Spectroscopy (FTIR) was used to identify functional groups and chemical bonds in the samples. Lastly, the sample was analyzed by Scanning Electron Microscopy (SEM) to examine its morphology and porosity. The SEM images revealed the material distribution and surface pores.

$$D = \frac{K \cdot \lambda}{\beta \cdot \cos \theta} \quad (1)$$

where;

D = crystallite size

K = shape factor (0.9)

λ = X-ray wavelength

β = line broadening (FWHM)

θ = Bragg angle

RESULTS AND DISCUSSION

The cockle shell was subjected to thermal analysis to determine at which point the decomposition of CaCO_3 to CaO has taken place. It was observed in Fig 2 that the cockle shell compound was completely decomposed to CO at 750°C . Prior to calcination, the cockle shells weighed 152.44 g, which then decreased to 148.35 g after the thermal regime. The weight loss of about ~ 2.68 wt% over the temperature range of $\sim 600^\circ\text{C}$ to 750°C could be attributed to decarboxylation of CaCO_3 , which is related to the release of carbon dioxide.

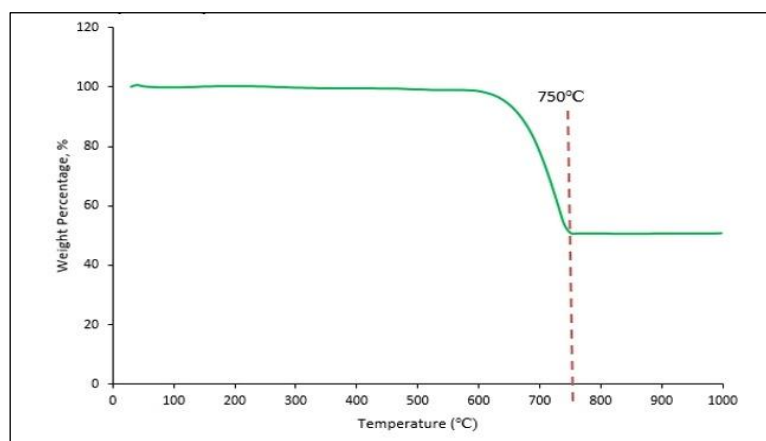


Fig. 2. TGA analysis of raw cockle shell.

Although Fig 2 shows that decomposition begins around 750°C , in this work, 800°C was regarded as the optimal conversion temperature from CaCO_3 to CaO . The thermal reaction of cockle shell which converts CaCO_3 into CaO was based on Equation 2.



Fig 3 shows the TGA analysis of the powder mixture of calcined cockle shell (CaO) and $(\text{NH}_4)_2\text{HPO}_4$. The observation implies that the full decomposition and phase transition have occurred at $\sim 785^\circ$, thus 800°C was regarded as the effective calcination temperature to obtain a pure crystalline form of HA with no other structural changes and degradation.

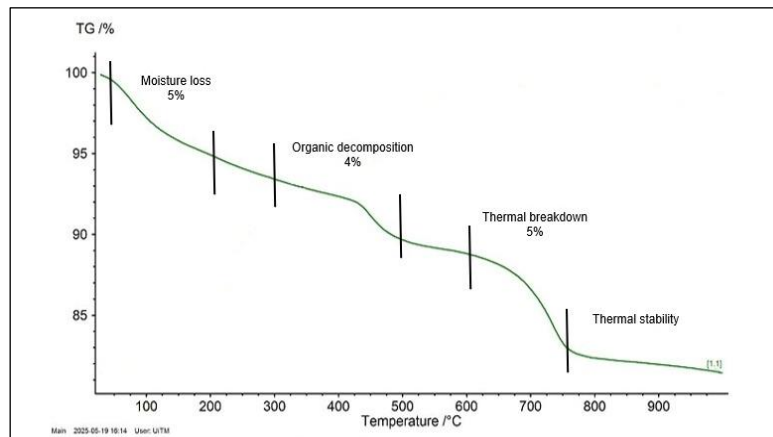


Fig. 3. TGA analysis of powder mixture (calcined cockle shell and $(\text{NH}_4)_2\text{HPO}_4$).

The formation of HA occurred through the following chemical reaction during the wet precipitation process, as shown in Equation 3.



Fig 4 shows the XRD traces of HA-PVA formation after being subjected to a sintering regime at 1000 °C. All HA-PVA samples show sharp XRD diffraction peaks at 2θ angles of 25.9°, 31.8°, 32.3°, 34.1° and 39.9°, which conform to the standard HA phase (JCPDS 09-0432). This trend supports the claim that sufficient heat from the calcination process has reduced any organic PVA bulk to pure HA phase (Indra et al., 2021). If the PVA does not fully combust, there are likely to be diffraction peaks associated with carbonic byproducts at lower angles (less than 20°). The relative peak intensities, as well as the peak profile on the plot in Fig 6 of HAP 3 (7.5 wt% PVA), were much stronger and sharper as compared to those of HAP 1 and HAP 2, indicating that HAP 3 was better crystallized and had more structures than the other two HA specimens sintered at this condition. The observations made are in accordance with reports of the mechanisms of thermal recrystallization seen in other comparable composite systems (Akram et al., 2023).

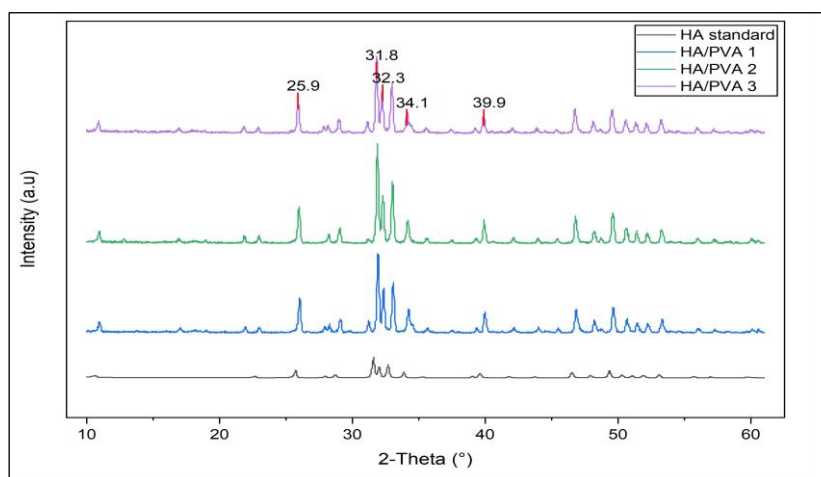


Fig. 4. XRD traces of HAP after sintering at 1000 °C.

<https://doi.org/10.24191/jmeche.v22i3.8194>

Table 2 shows the average crystallite size of HA calculated via the Scherrer equation (Equation 1). It was observed that the crystallite size shows an inverse correlation with peak intensity and PVA addition, whereby the size decreased with an increase in peak intensity and PVA content (Farias et al., 2019). Among the HA-PVA powders, HAP 3 shows the smallest crystallite (43.67 nm) and HAP 1 indicates the largest (47.25 nm). This finding has been supported by comparative studies; higher concentrations produce small grain size distributions since it enhances nucleation density and regulate grain growth during sintering (Gunawan et al., 2024). Hence, the XRD data show that the synthesis approach produced phase-pure HA with good crystallinity, and the calcination process successfully removed the PVA porogen without compromising the structure of HA (Kaniuk et al., 2023).

Table 2. Summary of the results for the average crystallite size

Sample	Average crystallite size (nm)
HAP 1	47.25
HAP 2	44.87
HAP 3	43.67

The FTIR spectrum of the HA-PVA powder is shown in Fig 5. Broad hydroxyl (OH) stretching vibrations are seen in all samples between 3000 cm^{-1} and 3600 cm^{-1} , indicating hydrogen bonding between PVA and HA (Hooi et al., 2021). The HAP 2 (5.0 wt% PVA) sample has the most distinct peak at 3435 cm^{-1} , indicating the best possible hydrogen bonding and stability (Xiang et al., 2022). The (PO_4^{3-}) vibrations, which are essential for the bioactivity of hydroxyapatite, are seen at 1022 cm^{-1} and 562 cm^{-1} . The HAP 2 has sharper peaks, indicating improved HA retention during sintering, while the carbonyl (C=O) and C-H stretching bands in the $1400\text{--}1700\text{ cm}^{-1}$ and $\sim 2900\text{ cm}^{-1}$ ranges further validate polymer integration (Zeng et al., 2011). The HAP 2 also has the most visible low-frequency bands at 472 cm^{-1} to 628 cm^{-1} , which correlate to O-P-O bending in HA which indicates improved crystallinity.

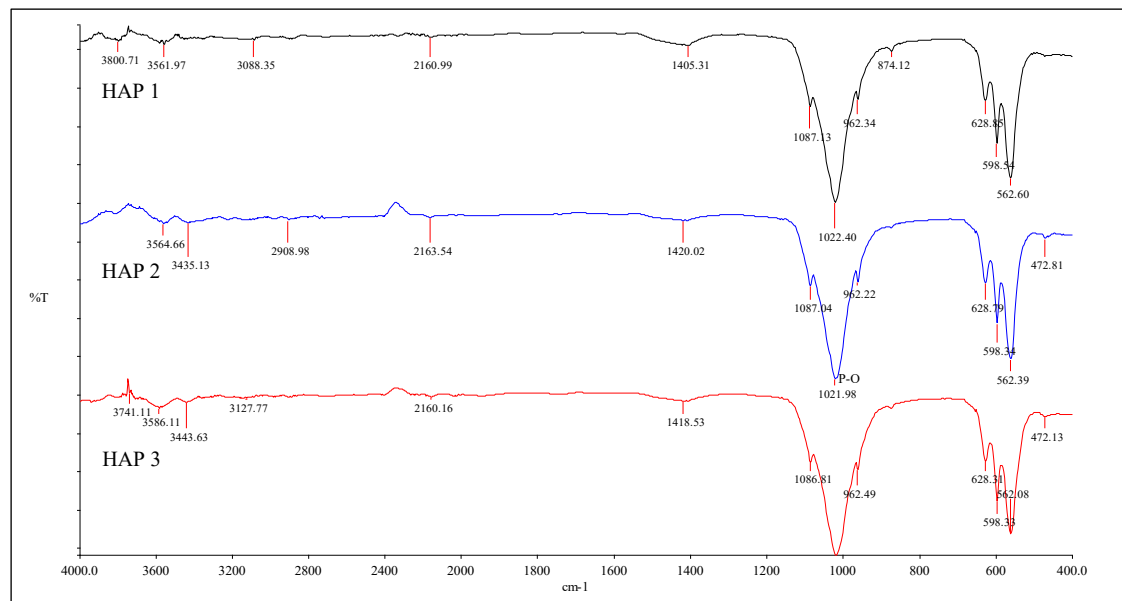


Fig. 5. FTIR spectra of HA-PVA at different PVA weight percentage.

Fig 6 shows SEM images of sintered HA-PVA composites containing 2.5 wt%, 5.0 wt%, and 7.5 wt% PVA. The images reveal significant variations in surface morphology and particle arrangement with increasing PVA content. It was observed that all HA-PVA samples have a globular particle shape. Meanwhile, the average particle size measured by the software ImageJ, as shown in Table 3, shows the particle decreased from 0.336 μm to 0.172 μm as the PVA concentration rises. This indicates that higher PVA content effectively reduces particle agglomeration. In addition, PVA acts as a dispersing and stabilizing agent by forming a polymeric coating around HA particles, limiting their tendency to stick together (Balgova et al., 2013). As the PVA content rises, the particles tend to become finer and more separated. This trend in particle size reduction is also reflected in the XRD results, where the average crystallite size slightly decreases with increasing PVA concentration from 47.25 nm in HAP 1 to 43.67 nm in HAP 3. The similarity in the decreasing trend of both particle size and crystallite suggests that PVA not only reduces surface agglomeration but may also influence the nucleation and growth process during synthesis, resulting in smaller, less crystalline domains (Antonova et al., 2024). Overall, increasing PVA concentration helps produce finer, more uniform HA particles with reduced agglomeration and slightly smaller crystallite sizes.

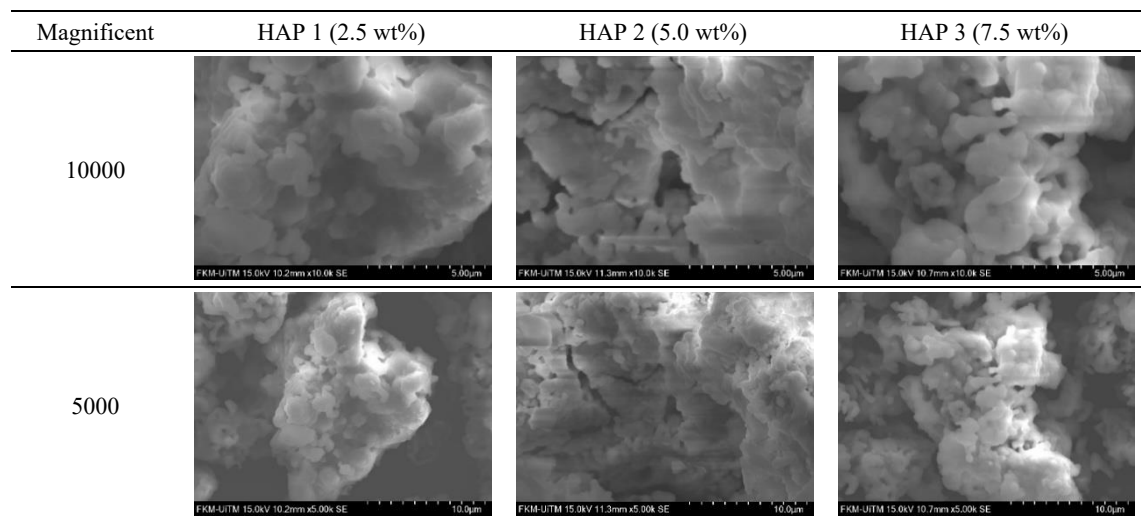


Fig. 6. SEM images of HA-PVA with varying PVA concentrations.

Table 3. Average particle size of HA-PVA with varying PVA concentrations

Sample	Average particle size (μm)
HAP 1	0.336
HAP 2	0.196
HAP 3	0.172

The results indicate that of the three samples, HAP 3 (7.5% PVA) shows the most positive characteristics. Despite having a reasonably high crystallinity with a crystallite size of 43.67 nm, it has the lowest degree of agglomeration and the smallest average particle size (0.172 μm), according to the SEM image. All the samples have the same globular shape. The HAP 3 (7.5% PVA) sample displayed the smallest average particle size (0.172 μm) and the most uniform dispersion, consistent with reduced agglomeration. In summary, the HA-PVA composites' structural quality is improved by the reduced agglomeration and smaller particle and crystallite sizes that result from an increase in PVA concentration

(Rajkumar et al., 2010). As a result, HAP 3 is regarded as the most homogeneous and structurally stable sample, yielding the best particle dispersion and crystal refinement results.

CONCLUSION

Hydroxyapatite (HA) using waste cockle shells as a calcium precursor has been successfully synthesized using the wet precipitation method and the effects of varying polyvinyl alcohol (PVA) concentrations on the properties of HA-PVA composites were determined. All samples formed pure, highly crystalline HA, according to XRD analysis, with the largest diffraction peak showing up at 31.8° at HAP 3 (7.5% PVA), which is consistent with conventional HA. Following sintering, the absence of any remaining PVA suggested that it had completely decomposed. Strong phosphate and hydroxyl group bands were visible in the FTIR spectra, indicating that HA had formed and that it had successfully interacted with PVA. SEM images showed that, especially at 7.5 wt% PVA, higher PVA concentrations resulted in finer globular morphology and reduced particle agglomeration. The findings confirmed that HA with 7.5 wt% PVA created a biocomposite that had the ideal ratio of structural homogeneity and crystallinity. This highlights the potential of using natural waste materials in developing sustainable and effective biomaterials for future biomedical applications.

ACKNOWLEDGEMENTS/ FUNDING

The authors would like to acknowledge the Ministry of Higher Education (MOHE) for funding under the Fundamental Research Grant Scheme (FRGS) (FRGS/1/2022/TK10/UITM/02/20) and the support of the Faculty of Mechanical Engineering, Universiti Teknologi MARA, Shah Alam, Selangor, Malaysia, for providing the facilities and financial support for this research.

CONFLICT OF INTEREST STATEMENT

The authors agree that this research was conducted in the absence of any self-benefits, commercial or financial conflicts and declare the absence of conflicting interests with the funders. One of the authors, Natasha Ahmad Nawawi, is the Section Editor of the Journal of Mechanical Engineering (JMEchE). The author has no other conflict of interest to note.

AUTHOR'S CONTRIBUTION

The authors confirm their contribution to the paper as follows: **study conception and design:** Anis Fadhilla Azhar, Nur Hezreen Najwa Abdul Muizz, Natasha Ahmad Nawawi; **data collection:** Anis Fadhilla Azhar, Nur Hezreen Najwa Abdul Muizz; **analysis and interpretation of results:** Anis Fadhilla Azhar, Nur Hezreen Najwa Abdul Muizz, Natasha Ahmad Nawawi; **draft manuscript preparation:** Anis Fadhilla Azhar, Natasha Ahmad Nawawi. All authors reviewed the results and approved the final version of the manuscript.

REFERENCE

- Abifarin, F. B., Musa, Z., & Abifarin, J. K. (2023). Mechanical processing of hydroxyapatite through sintering and multi-objective optimization technique for biomedical application. *MRS Advances*, 8(9), 532-537.
- Akram, W., Khan, R., Amjad, M., Muhammad, R., & Yasir, M. (2023). Densification of nanocrystalline hydroxyapatite powder via sintering: Enhancing mechanical properties for biomedical applications. *Materials Research Express*, 10(7), 075402.
- Anggresani, L., Nurmelinda, Yulianis, & Lim, L. W. (2023). Utilizing Anadara granosa shells and PVA for porous hydroxyapatite synthesis. *Indonesian Journal of Chemical Engineering*, 1(2), 86-94.
- Antonova, O. S., Goldberg, M. A., Fomin, A. S., Kucheryaev, K. A., Kononov, A. A., Sadovnikova, M. A., Murzakhanov, F. F., Sitnikov, A. I., Leonov, A. V., Andreeva, N. A., Khayrutdinova, D. R., Gafurov, M. R., Barinov, S. M., & Komlev, V. S. (2024). Meso-macroporous hydroxyapatite powders synthesized in polyvinyl alcohol or polyvinylpyrrolidone media. *Nanomaterials*, 14(16), 1338.
- Balgová, Z., Palou, M., Wasserbauer, J., & Kozánková, J. (2013). Synthesis of poly (vinyl alcohol)-hydroxyapatite composites and characterization of their bioactivity. *Central European Journal of Chemistry*, 11(9), 1403-1411.
- Cahyaningrum, S. E., Herdyastuty, N., Devina, B., & Supangat, D. (2018). Synthesis and characterization of hydroxyapatite powder by wet precipitation method. *IOP Conference Series: Materials Science and Engineering*, 299, 012039.
- Cruz-Ávila, C., Hernández-Padrón, G., & Meneses, V. M. C. (2024). Sonochemistry-assisted sol-gel synthesis of hydroxyapatite [Preprint]. *Research Square*. <https://doi.org/10.21203/rs.3.rs-5398412/v1>
- Farias, K. A. S., Sousa, W. J. B., Cardoso, M. J. B., Lima, R. J. S., Rodriguez, M. A., & Fook, M. V. L. (2019). Obtaining hydroxyapatite with different precursors for application as a biomaterial. *Cerâmica*, 65(373), 99-106.
- Gunawan, Arifin, A., Yani, I., Oemar, B., Sudarsono, Ramli, M. I., & Wijayanto, I. G. (2024). Preparation and characterization of hydroxyapatite based composite material via cold sintering process. *Journal of Advanced Research in Micro and Nano Engineering*, 21(1), 127-136.
- Hooi, M. T., Phang, S. W., Yow, H. Y., David, E., Kim, N. X., & Choo, H. L. (2021). FTIR spectroscopy characterization and critical comparison of poly (vinyl) alcohol and natural hydroxyapatite derived from fish bone composite for bone-scaffold. *Journal of Physics: Conference Series*, 2120, 012004.
- Indra, A., Gunawarman, Affi, J., Mulyadi, I. H., & Wiyanto, Y. (2021). Physical and mechanical properties of hydroxyapatite ceramics with a mixture of micron and nano-sized powders: Optimising the sintering temperatures. *Ceramics-Silikaty*, 65(3), 224-234.
- Italiano, A. E. V., Tranquilin, R. L., Marin, D. O. M., Santos, M. L., & Vaz, L. G. (2024). Synthesis of calcium phosphate by microwave hydrothermal method: Physicochemical and morphological characterization. *International Journal of Biomaterials*, 2024, 2167066.
- Kaniuk, E., Lechowska-Liszka, A., Gajek, M., Nikodem, A., Ścisłowska-Czarnecka, A., Rapacz-Kmita, A., & Stodolak-Zych, E. (2023). Correlation between porosity and physicochemical and biological properties of electrospinning PLA/PVA membranes for skin regeneration. *Biomaterials Advances*, 152, 213506.
- Kati, N., Ozan, S., Yildiz, T., & Arslan, M. (2022). Effect of reaction time and heat treatment in the <https://doi.org/10.24191/jmeche.v22i3.8194>

- production of hydroxyapatite by hydrothermal synthesis. *Archives of Metallurgy and Materials*, 67(4), 1427-1434.
- Khiri, M. Z. A., Matori, K. A., Zainuddin, N., Abdullah, C. A. C., Alassan, Z. N., Baharuddin, N. F., & Zaid, M. H. M. (2016). The usability of ark clam shell (*Anadara granosa*) as calcium precursor to produce hydroxyapatite nanoparticle via wet chemical precipitate method in various sintering temperature. *SpringerPlus*, 5, 1206.
- Ng, C. K., Lee, K. Y. S., Tan, C. H., Ramesh, S., Ting, C. H., Chuah, Y. D., Tan, C. Y., & Sutharsini, U. (2022). Characterization and sintering properties of hydroxyapatite bioceramics synthesized from clamshell biowaste. *IIUM Engineering Journal*, 23(2), 228-236.
- Novella, I., Rupaedah, B., Eddy, D. R., Suryana, Irwansyah, F. S., & Noviyanti, A. R. (2023). The influence of polyvinyl alcohol porogen addition on the nanostructural characteristics of hydroxyapatite. *Materials*, 16(18), 6313.
- Priwintoko, B., Ismail, R., Fitriyana, D. F., Subagyo, Y., & Bayuseno, A. P. (2023). Effect of sintering temperature and polyvinyl alcohol composition as binder on the formation of porous hydroxyapatite as bone graft using sponge replication method: A review. *Mechanical Engineering for Society and Industry*, 3(3), 136-151.
- Rajkumar, M., Sundaram, N. M., & Rajendran, V. (2010). In-situ preparation of hydroxyapatite nanorod embedded poly (vinyl alcohol) composite and its characterization. *International Journal of Engineering Science and Technology*, 2(6), 2437-2444.
- Redhwi, I., Fallatah, A., & Alshabona, F. (2024). Hydroxyapatite: A comprehensive review of its properties, applications, and future trends. *International Journal of Biomedical Materials Research*, 12(1), 1-6.
- Rosley, R., Badarulzaman, N. A., Suradi, S. S., & Dzinun, H. (2024). Preparation and characterization of hydroxyapatite using precursor extracted from cockle shell waste. *PaperASIA*, 40(4b), 248-253.
- Shalygina, K., Lytkina, D., Sadykov, R., & Kurzina, I. (2024). Composite cryogels based on hydroxyapatite and polyvinyl alcohol and the study of physicochemical and mechanical properties. *Materials*, 17(2), 403.
- Sirisoam, T., Saelee, C., Thiansem, S., & Punyanitya, S. (2018). Characteristic, microstructure and properties of dense hydroxyapatite ceramic from cockle shell for biomaterials. *Materials Science Forum*, 940, 3-7.
- Trzaskowska, M., Vivcharenko, V., & Przekora, A. (2023). The impact of hydroxyapatite sintering temperature on its microstructural, mechanical, and biological properties. *International Journal of Molecular Sciences*, 24(6), 5083.
- Xiang, C., Zhang, X., Zhang, J., Chen, W., Li, X., Wei, X., & Li, P. (2022). A porous hydrogel with high mechanical strength and biocompatibility for bone tissue engineering. *Journal of Functional Biomaterials*, 13(3), 140.
- Zeng, S., Fu, S., Guo, G., Liang, H., Qian, Z., Tang, X., & Luo, F. (2011). Preparation and characterization of nano-hydroxyapatite/poly (vinyl alcohol) composite membranes for guided bone regeneration. *Journal of Biomedical Nanotechnology*, 7(4), 549-557.